AIP | Journal of Applied Physics

Discrimination between coupling and anisotropy fields in exchange-biased bilayers

J. Geshev, S. Nicolodi, R. B. da Silva, J. Nogués, V. Skumryev, and M. D. Baró

Citation: Journal of Applied Physics **105**, 053903 (2009); doi: 10.1063/1.3079795
View online: http://dx.doi.org/10.1063/1.3079795
View Table of Contents: http://scitation.aip.org/content/aip/journal/jap/105/5?ver=pdfcov
Published by the AIP Publishing

Discrimination between coupling and anisotropy fields in exchange-biased bilayers

J. Geshev,[1,a)] S. Nicolodi,[1] R. B. da Silva,[2] J. Nogués,[3,4] V. Skumryev,[3,5] and M. D. Baró[5]
[1]*Instituto de Física, Universidade Federal do Rio Grande do Sul (UFRGS), Porto Alegre, 91501-970 Rio Grande do Sul, Brazil*
[2]*Centro de Ciências Exatas e Tecnológicas, Universidade Federal do Pampa (UNIPAMPA), Caçapava do Sul, 96570-000 Rio Grande do Sul, Brazil*
[3]*Institució Catalana de Recerca i Estudis Avançats (ICREA), 08010 Barcelona, Spain*
[4]*Centre d'Investigacions en Nanociència i Nanotecnologia (ICN-CSIC), Campus de la Universitat Autònoma de Barcelona, Bellaterra, 08193 Barcelona, Spain*
[5]*Departament de Física, Universitat Autònoma de Barcelona, Bellaterra, 08193 Barcelona, Spain*

(Received 26 November 2008; accepted 7 January 2009; published online 3 March 2009)

In the framework of models that assume planar domain wall formed at the antiferromagnetic part of the interface of exchange-biased bilayers, one cannot distinguish between the cases of high or low ratios between the coupling and the antiferromagnet's anisotropy fields by using hysteresis loop measurement, ferromagnetic resonance, anisotropic magnetoresistance, or ac susceptibility techniques applied on one and the same sample. The analysis of the experimental data obtained on a series of FeMn/Co films indicated that once the biasing is established the variation in the coercivity with the FeMn layer thickness could be essential for solving this problem. If the coercivity decreases with the thickness then the interlayer exchange coupling is the parameter that varies while the domain-wall energy of the antiferromagnet remains practically constant. © *2009 American Institute of Physics*. [DOI: 10.1063/1.3079795]

I. INTRODUCTION

In the last two decades there has been a remarkable interest in the exchange-bias (EB) effect[1,2] which results from the magnetic coupling between a ferromagnet (FM) and a small fraction of partially uncompensated interfacial spins in an adjacent antiferromagnet (AF). By definition, these are moments of atoms in an AF atomic plane which sum up to give a nonvanishing net magnetization in that plane. The uncompensated moments could point in the FM magnetization direction either after a field cooling procedure or if the AF is deposited in the presence of magnetic field or after ion bombardment in such a field. If these spins do not rotate upon switching the FM magnetization, they will lead to EB.

Despite the vast number of experimental and theoretical investigations,[3–7] several controversial issues concerning this phenomenon still exist. Among them is the fact that different measurement techniques may yield distinct values[8–20] for the FM/AF exchange coupling constant J_E, being these differences of up to one order of magnitude. This has lead some authors to classify the techniques in two categories: reversible and irreversible.[15] For example, the ferromagnetic resonance (FMR), Brillouin light scattering, and ac magnetic susceptibility techniques involve only small perturbations of the magnetization around equilibrium, while hysteresis loop and torque measurements involve irreversible switching of the FM magnetization.

J_E is estimated by comparing experimental data with those calculated in the framework of a properly chosen phenomenological model. The majority of the works reporting discrepancies between the coupling energies estimated through different techniques have adopted either the rigid AF moment (RAF) model which assumes that the AF moment $\mathbf{M}_{AF}$ always points along its original pinning direction or a model that allows a domain-wall formation (DWF) at the AF part of the FM/AF interface.[21] If the AF anisotropy is very high, the more general and flexible DWF model is reduced to the former one. When the AF is sufficiently thick, the DWF model itself turns to be a particular case of that proposed by Xi and White[22] for a bilayer of finite AF thickness.

In the present study, another problem concerning the determination of J_E is pointed out. We show that even when the DWF model describes correctly an EB bilayer, none of the conventional reversible or irreversible techniques, applied to the same sample, is capable to distinguish between the exchange coupling and the AF anisotropy fields if their ratio is sufficiently high or low. In order to shed light on this dilemma, a series of FeMn/Co bilayers, where the FeMn layer thickness t_{AF} is varied, is investigated as a probe system. It is demonstrated that, provided the proposed scenario is consistent with the system under investigation, the values of J_E can be properly determined with the help of the variation in the coercivity with t_{AF}.

II. THEORETICAL CONSIDERATIONS

Here we adopt a modified DWF model described in Appendix A. In the framework of this model, by finding the equilibrium directions of $\mathbf{M}_{FM}$ and $\mathbf{M}_{AF}$, one can numerically simulate magnetization curves,[14,16,18–20,23] transverse-biased ac susceptibility[20] χ_t, FMR field[16,18,19] H_R, and anisotropic magnetoresistance (AMR) (Ref. 24) for any in-plane dc field direction given by ϕ_H. Representative hysteresis loop's field shift H_{eb}^{MAG} (extracted from the simulated loops) as well as

a)Electronic mail: julian@if.ufrgs.br.

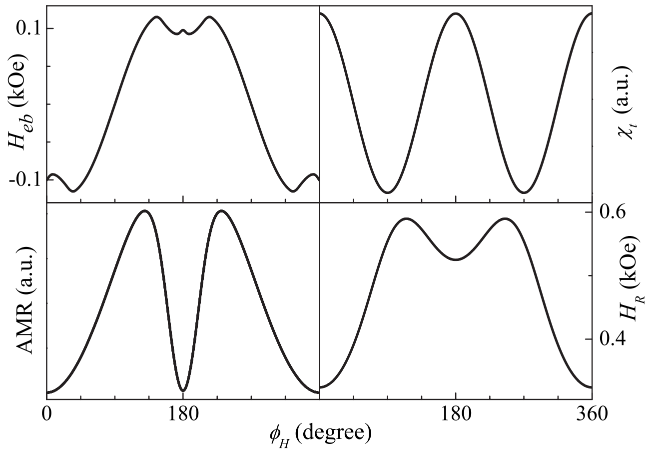

FIG. 1. Representative H_{eb}^{MAG}, χ_t, AMR (in-plane electric current perpendicular to the easy axis, $H=100$ Oe) and H_R as functions of ϕ_H calculated using $M_{\mathrm{FM}}=1400$ emu/cm^3, $H_U=80$ Oe, $H_{\mathrm{RA}}=0$ Oe, $\omega/\gamma=3$ kOe (here ω is the angular frequency of precession and γ is the FM layer gyromagnetic ratio), $H_W=1500$ Oe, and $H_E=100$ Oe. Practically the same curves are obtained if the values of H_W and H_E are interchanged, i.e., $H_W=100$ Oe and $H_E=1500$ Oe.

χ_t, AMR, and H_R angular variations are given in Fig. 1. The parameters used in the simulations are given in the caption of the figure. These are the exchange coupling field $H_E = J_E/(t_{\mathrm{FM}}M_{\mathrm{FM}})$, the AF domain-wall anisotropy field $H_W = \sigma_W/(t_{\mathrm{FM}}M_{\mathrm{FM}})$, where σ_W is the energy per unit surface of a 90° AF domain wall, and the FM anisotropy field $H_U = 2K_{\mathrm{FM}}/M_{\mathrm{FM}}$ of the FM layer with uniaxial anisotropy constant K_{FM} and thickness t_{FM}. It is worth noting that H_E does not coincide with H_{eb}^{MAG} since the latter, in general,[14] also depends on K_{FM} and on the AF anisotropy constant K_{AF}. The rotatable anisotropy field H_{RA} accounts for spins at the AF part of the FM/AF interface which switch together with the FM magnetization. The coupling with these AF spins is effectively sensed by the FM as an additional uniaxial anisotropy parallel to **H**, leading to an enhancement not of the EB field but of H_C. Detailed definition of the rotatable anisotropy field H_{RA} is given in Appendix A.

Curves *identical* to those shown in Fig. 1 are also obtained when the values of H_E and H_W are interchanged. This fact could be understood considering, e.g., the expressions for χ_t derived[17] for $\phi_H=0$, $\pi/2$, and π for both cases of H_E smaller or bigger than H_W, which turn to be the same when interchanging H_E and H_W. In the limits of very small and very big H_E/H_W ratios one gets an identical situation for the easy axis EB field since it equals H_E when H_E/H_W is very small while very big ratio corresponds to $H_{eb}^{\mathrm{MAG}}=H_W$. In both cases, the hysteresis loop shift equals the smaller (domain-wall anisotropy or exchange coupling) field.[14,21]

Also, for H_E/H_W lower than a certain value,[14] the easy axis coercivity, H_C, is

$$H_C = H_U + H_{\mathrm{RA}} - \frac{H_E^2 H_W}{H_W^2 - H_E^2}, \tag{1}$$

while for H_E/H_W bigger than a certain value it is

$$H_C = H_U + H_{\mathrm{RA}} - \frac{H_W^2 H_E}{H_E^2 - H_W^2}. \tag{2}$$

Again, one and the same H_C is obtained when interchanging H_E and H_W. Consequently, the above cited techniques, applied on an exchange-biased bilayer at a certain temperature, cannot distinguish between H_E and H_W if their ratio is sufficiently big or small. Since both fields vary with the temperature, T, we checked the possibility H_E and H_W to become comparable within a certain temperature range, which would thus permit to decide which of them is bigger at the initial measurement temperature. Theoretical H_E, H_W, and H_E/H_W dependencies on T are shown in Appendix B. It is seen that although H_E/H_W increases with the temperature, H_E and H_W are comparable only for $H_E < H_W$ and for T very close to T_N. Unfortunately, this makes the tryout to distinguish between high and low H_E/H_W ratios by varying T inviable since close to T_N the EB field is very small leading to big error margin in the anisotropy parameters' estimation.

The above considerations indicate that one has to modify in a controllable manner either H_E or H_W and to find a way to identify the parameter that has been modified. For this purpose, we studied a series of FM/AF films where the thickness of the AF layer has been varied.

III. EXPERIMENTAL

Ta(5 nm)/FeMn(t_{AF})/Co(10 nm)/Ta(5 nm) films, where t_{AF} is varied between 2 and 6 nm, were deposited onto Si(100) substrates by dc magnetron sputtering with base pressure of 5.0×10^{-7} Torr and Ar pressure of 2×10^{-3} Torr. In order to enhance the EB field, the films were slowly cooled from 250 °C to room temperature in vacuum of 5.0×10^{-6} Torr with magnetic field of 3.5 kOe applied in the plane of the films. This series of samples was chosen for the present study due to the gradual and not very steep increase in H_{eb}^{MAG} at room temperature[25] for t_{AF} varying between 3 and 6 nm thus allowing us to grow samples with different anisotropy parameters. The magnetic characterization, unless otherwise stated, was done at room temperature using alternating gradient-field magnetometer with **H** applied in the plane of the films.

IV. RESULTS AND DISCUSSION

Easy-axis hysteresis loops for the samples with $t_{\mathrm{AF}}=3$, 4, 5, and 6 nm for **H** applied along the easy direction are shown in Fig. 2. The AF thickness dependencies of the experimentally obtained H_{eb}^{MAG} and H_C as well as the parameters used for the fitting curves plotted in this figure are given in Fig. 3. The rounded shape of the magnetization curves indicates that the FM/AF interface is partly disordered which, in the model simulations, is taken into account by considering certain distributions[19,20,23,26] of $\hat{\mathbf{u}}_{\mathrm{FM}}$ and $\hat{\mathbf{u}}_{\mathrm{AF}}$ (see the caption of Fig. 2). Note that the expressions for H_C given by Eqs. (1) and (2) are valid for the case of a single FM/AF pair with **H** parallel to the EB direction; considering the above easy axis distributions may result in H_C much lower than H_U+H_{RA}.

The H_{eb}^{MAG} and H_C trends are typical of those found in the literature for the Co/FeMn system[25,27] where the onset of

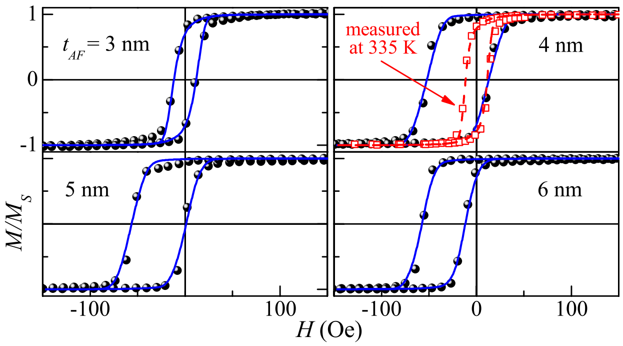

FIG. 2. (Color online) Easy-axis magnetization curves for the samples with $t_{\rm AF}$=3, 4, 5, and 6 nm at 298 K. The lines are fitting curves obtained using H_U=20 Oe, the effective fields from Fig. 3, FM easy axis distribution with 65° maximum deviation away from the easy direction and standard deviation of 200°, as well as equally distributed in-plane $\hat{\mathbf{u}}_{\rm AF}$ unit vectors with 25° maximum deviation away from ϕ_H=0. When a value for H_E from Fig. 3 is used, then H_W=500 Oe is employed and vise versa. The open squares in the panel for $t_{\rm AF}$=4 nm are the respective data measured at 335 K showing H_C=11 Oe and no field shift (the fitting dashed curve is obtained using only H_U=20 Oe and the above cited FM easy axis distribution).

biasing (i.e., $H_{eb}^{\rm MAG} \neq 0$) appears at $t_{\rm AF} > 3$ nm and $H_{eb}^{\rm MAG}$ reaches its saturation at about 8 nm. Our limit for the onset of biasing (≈4 nm) is in excellent agreement with the data of Offi *et al.*[27] when assuming FeMn lattice parameter[28] a =3.63 Å, which results in the thickness of approximately 11 MLs. One might argue that this is the point where the transition from paramagnetic to AF state occurs for FeMn. However, since we measured 40% higher coercivity for $t_{\rm AF}$ =3 nm than that for $t_{\rm AF}$=2 nm before the appearance of any biasing (i.e., FeMn is already behaving as an AF), it seems that 4 nm is a thickness at which the AF is capable to accommodate a planar domain wall (see below).

It is very difficult to detect magnetic domains within the AF layer in an exchange-coupled system. The first indirect evidence of a spiraling AF spin structure has been observed by Yang and Chien[29] in an FeMn film sandwiched between $Ni_{81}Fe_{19}$ and Co pointing to the validity of the DWF model.

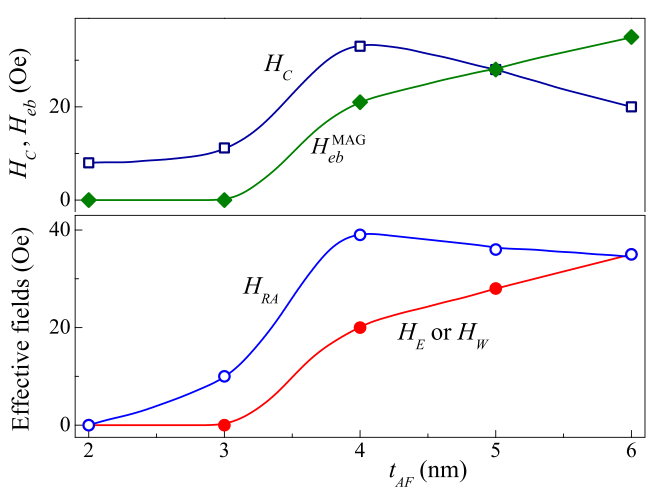

FIG. 3. (Color online) AF thickness dependencies of the experimentally measured $H_{eb}^{\rm MAG}$ and H_C (top panel) and of the parameters used for fitting the curves in Fig. 2 keeping H_U=20 Oe (bottom panel). The $H_{eb}^{\rm MAG}$ and H_C values extracted from the simulated hysteresis loops coincide with the experimental ones. The lines are guides for the eyes.

The experimental detection of interfacial AF domains is very difficult and has only been achieved in very special cases.[30,31] The good agreement between model and experiment seen in Fig. 2, however, indicates that our data could be interpreted in terms of domain walls formed at the AF side of the interface.[21] Although the thickness of ≈4 nm may seem to be rather low to accommodate planar walls, in the next paragraph we present some reasoning that such walls may, in fact, be formed.

Ali *et al.*[25] estimated that FeMn layers of thickness like ours are too thin to support a planar parallel wall since domain-wall width δ_W $(=\frac{\pi}{2}\sqrt{A_{\rm AF}/K_{\rm AF}}$, where $A_{\rm AF}$ is the AF exchange stiffness) of 28 nm is obtained using the value of 430 K for the Néel temperature of FeMn and $K_{\rm AF}$=1.3 $\times 10^5$ erg/cm^3. However, there is a progressive reduction in the Néel temperature due to the finite-size scaling[32] and at the thickness for the onset of biasing the AF ordering temperature is very close to room temperature for FeMn.[27] Our sample with $t_{\rm AF}$=4 nm, when measured at temperatures higher than 335 K, shows unbiased hysteresis loops (the curve obtained at 335 K is plotted in Fig. 2). Employing 335 K instead of T_N for calculation of $A_{\rm AF}$ together with $K_{\rm AF}$ =3.0×10^6 erg/cm^3 as recently estimated,[33] one obtains δ_W =5.1 nm, a value close to $t_{\rm AF}$ of our sample with thinnest FeMn layer with nonzero $H_{eb}^{\rm MAG}$. The lower FeMn anisotropy values estimated earlier (e.g., in the work of Mauri *et al.*[21]) could be ascribed to thermal activation processes occurring during the measurements at high temperatures.[34,35]

Interface defects may lower the symmetry of the crystal fields thus leading to enhancement in the anisotropy due to local structural deformations and associated elastic strains.[36] This strain-related interface anisotropy can be up to an order of magnitude larger than the corresponding bulk value for moderate strains. Increase in $K_{\rm AF}$ due to stoichiometric changes in the bulk of the NiO layer has been reported.[37] Modifications of the anisotropy energy also affect the energy required to form the wall; interfacial defects reduce H_E and bulk defects in the AF lower the average exchange energy in the AF, $J_{\rm AF}$, thereby reducing the cost of forming a partial wall[36] since $\sigma_W \propto A_{\rm AF} \simeq J_{\rm AF}/a$. Let us now focus our attention on the main problem, i.e., the apparent impossibility to discriminate between low and high H_E/H_W ratios using only one sample and see if the individual variations in H_E and H_W with $t_{\rm AF}$ would permit one to solve the dilemma.

Our numerical simulations of the experimental data gave that one of H_E and H_W varies between 0 and 35 Oe when $t_{\rm AF}$ is increased from 0 to 6 nm, while the other has the much bigger and practically constant value of 500 Oe. Let us assume that the parameter that changes is H_W. Using $t_{\rm FM}$ =10 nm and the literature value for the Co saturation magnetization $M_{\rm FM}$=1400 emu/cm^3, the estimated σ_W =$t_{\rm FM}M_{\rm FM}H_W$ varies between 0 and 0.05 erg/cm^2. The latter value is approximately eight times lower than that normally found in the literature[21] and 38 times lower than σ_W =$\sqrt{A_{\rm AF}K_{\rm AF}}$ calculated when employing $A_{\rm AF}$ and $K_{\rm AF}$ used in the above δ_W(=5.1 nm) estimation. The respective exchange coupling constant J_E=$t_{\rm FM}M_{\rm FM}H_E$ turns to be 0.7 erg/cm^2

using H_E=500 Oe, while the upper end of the range of J_E reported in the literature[3] for sputtered FeMn films is 0.2 erg/cm^2.

Due to somewhat unphysical values of the parameters derived from H_E and H_W, we conclude that J_E is the parameter that increases with t_{AF} (i.e., 0.05 erg/cm^2 for t_{AF} =6 nm) while the constant one is σ_W=0.7 erg/cm^2. These values are in a good agreement with the literature data. This discrimination between H_E and H_W, however, was done from comparison with already published results instead of using their thickness variations. In fact, this could well be done using only one of the samples.

In what follows we show that, if the enhancement of H_C is due to antiferromagnetism of the bilayer and if the proposed here scenario is consistent with the system under investigation, one can distinguish between H_E and H_W even for a bilayer with unknown exchange coupling or anisotropy characteristics with the help of the experimentally measured $H_C(t_{AF})$ and the estimated from the fittings $H_{RA}(t_{AF})$.

Figure 3 shows that the coercivity initially increases, attains its maximum at t_{AF} for which biasing first occurs, and then gradually decreases, which is accompanied by an enhancement of the EB field. The values of H_C and H_{eb}^{MAG} extracted from the fitted hysteresis loops coincide with the experimental ones. As mentioned above, the initial increase in H_C without biasing at t_{AF}=3 nm indicates that AF order is already established and that certain fraction of frustrated spins in the FeMn rotates reversibly with the FM magnetization during the measurement of a hysteresis loop. The increase in H_C close to the AF thickness for onset of biasing could alternatively be attributed to imperfections in the AF, e.g., embedded impurities or crystal defects, irreversible transitions of grains,[38] to pinning the partial wall formed in the AF,[36] interfacial magnetic frustration,[39] or to regions with locally different blocking temperatures[40] depending on t_{AF}. Despite that FeMn is already behaving as an AF, at t_{AF} =3 nm it is still not capable to accommodate a planar domain wall, resulting in zero field shift. The quite opposite trends of $H_C(t_{AF})$ and $H_{eb}^{MAG}(t_{AF})$ for $t_{AF} \geq 4$ nm confirm that these variations are due to changes at the FM/AF interface, i.e., the raise of H_{eb}^{MAG} comes from the increasing number of stable AF domains at expense of AF moments dragged during a hysteresis loop trace.

In our case, the terms containing H_E and H_W in Eqs. (1) and (2) are very small as compared to H_U+H_{RA} so the variation in H_C is effectively given by that of H_{RA} taking for granted that H_U, which is an intrinsic property of the FM layer, does not change with t_{AF}. This particular property is essential for the discrimination between H_E and H_W. It is worth recalling that the visibly lower variation in H_C as compared to that of H_{RA} seen in Fig. 3 is due to local noncollinearity between the $\hat{\mathbf{u}}_{FM}$ and $\hat{\mathbf{u}}_{AF}$ vectors, taken into account by considering their in-plane distributions. One could also expect modifications of the latter with the AF thickness.[37] Our simulations, however, did not indicate significant variations in these distributions.

Magnetic moments at surface terrace edges and surface defects play a decisive role because noncollinearities between spins in the surface and the bulk may exist during magnetization reversal. These spins can be considered as "loose spins" with weakened exchange interaction at the surface and from defects.[41] On the other hand, upon increasing the AF film thickness the number of bulk inhomogeneities, e.g., structural, thickness, or compositional randomness, in the AF layer is increased leading to more effective pinning of the AF spin configuration and to biasing.[42] Thus, starting from the AF thickness that corresponds to the onset of biasing, the number of stable AF domains grows with t_{AF} while the AF spins that can irreversibly switch their magnetizations decrease in number. Hence H_{RA}, which reflects exclusively the latter type of AF moments, also decreases.

As already mentioned, the AF ordering temperature is reduced for very thin AF layers due to finite-size effects, resulting in low values of A_{AF}. Conversely, increasing t_{AF} tends to enhance A_{AF}; hence, J_{AF} increases ($J_{AF} \simeq aA_{AF}$) and so does the effective FM/AF coupling which is proportional to $\sqrt{J_{AF}}$. Thus, the model should estimate growing $H_E(t_{AF})$; negative variation in H_C should also be experimentally obtained since H_{RA} decreases with t_{AF} due to the decrease in number of the unstable (i.e., "rotatable") AF spins. Both features were observed here sustaining the assumption that the smaller (and variable with t_{AF}) parameter is H_E. The variation in the AF domain-wall anisotropy, if any, is insignificant as compared to that of the effective exchange coupling.

Due to the unavailability of experimental data for AF domain-wall formation, it is worth commenting on the validity of the conclusions drawn for the considered here scenario, i.e., direct exchange interactions without AF domain walls for $t_{AF} \simeq 3$ nm and both direct exchange and domain walls for $t_{AF} \geq 4$ nm. An alternative explanation for the H_{eb}^{MAG} variation could be that for AF thickness below 4 nm the FeMn layer is paramagnetic; above 4 nm there is no wall formation since t_{AF} is too small and the hysteresis loop's shift comes from direct exchange of pinned spins in the AF layer as proposed in the partial wall model of exchange bias.[36] In such a case the formation of a AF domain wall costs too much energy and the responsible for the bias AF moments point always along the pinning direction. This condition may be viewed in terms of the RAF model which, as mentioned above, is a particular case of the DWF model, that of very high σ_W, even for distributed $\hat{\mathbf{u}}_{AF}$ directions. In this case, the discrimination between H_E and H_W is straightforward since the AF anisotropy term in the energy expression is constant and very high. Consequently, the H_E/H_W ratio is very low and the model gives J_E directly.

In summary, we showed that using hysteresis loop measurement, FMR, AMR, or ac susceptibility techniques applied on one and the same sample one cannot distinguish between the cases of high or low ratios between the exchange coupling and the AF anisotropy fields, even when the model employed in the interpretation of the experiment correctly describes the system. The analysis of the experimental data obtained on a series of FeMn/Co bilayers where the AF layer thickness was varied pointed out that the coercivity variation could be essential for solving this problem. If the coercivity decreases with the AF layer thickness when the latter is higher than that corresponding to the onset of biasing, then the FM/AF coupling is the parameter that changes.

ACKNOWLEDGMENTS

J.G. thanks S. Rioual for pointing out the problem which has motivated the present work and acknowledges the sabbatical fellowship (Grant No. SAB2006-0193) from the Spanish Ministry of Science and Education. This work has also been supported by the Brazilian agency CNPq (project nos. 300945/2006-0 and 477266/2006-1) as well as by the DGR (Catalan Government) and the CICYT (Spanish Government) through project nos. 2005GR-00401 and MAT-2007-66302-C02.

APPENDIX A: DWF MODEL

In the framework of the DWF model, the free magnetic energy per unit area can be written as

$$E = 2\pi(\mathbf{M}_{\mathrm{FM}}\cdot\hat{\mathbf{n}})^2 - \mathbf{H}\cdot\mathbf{M}_{\mathrm{FM}}t_{\mathrm{FM}} - K_{\mathrm{FM}}t_{\mathrm{FM}}\left(\frac{\mathbf{M}_{\mathrm{FM}}\cdot\hat{\mathbf{u}}_{\mathrm{FM}}}{M_{\mathrm{FM}}}\right)^2 - \sigma_W\frac{\mathbf{M}_{\mathrm{AF}}\cdot\hat{\mathbf{u}}_{\mathrm{AF}}}{M_{\mathrm{AF}}} - J_E\frac{\mathbf{M}_{\mathrm{FM}}\cdot\mathbf{M}_{\mathrm{AF}}}{M_{\mathrm{FM}}M_{\mathrm{AF}}} - K_{\mathrm{RA}}t_{\mathrm{FM}}\left(\frac{\mathbf{M}_{\mathrm{FM}}\cdot\hat{\mathbf{h}}}{M_{\mathrm{FM}}}\right)^2.$$

Here, the first three terms are the FM demagnetizing, Zeeman, and uniaxial anisotropy energies, respectively, the forth term is the AF anisotropy, the fifth term is the bilinear exchange coupling energy, and the last term is the rotatable anisotropy[23] being K_{RA} its anisotropy constant. The unit vectors $\hat{\mathbf{n}}$, $\hat{\mathbf{h}}$, $\hat{\mathbf{u}}_{\mathrm{FM}}$, and $\hat{\mathbf{u}}_{\mathrm{AF}}$ represent the normal to the film's surface direction, the applied dc field direction, the FM uniaxial anisotropy direction, and the original pinning direction of the AF, respectively; t_{FM} is the thickness of the FM with saturation magnetization M_{FM} and anisotropy constant K_{FM}.

It is accepted that a domain wall or a partial domain wall forms in the AF parallel to the FM/AF interface as the FM rotates since it is energetically more favorable to deform the AF magnetic structure rather than breaking the interfacial coupling. This mechanism is only possible if the AF layer is of thickness at least sufficient to accommodate a planar domain wall.

When the model was first proposed,[21] it was supposed that $\mathbf{H}$, $\hat{\mathbf{u}}_{\mathrm{FM}}$, and $\hat{\mathbf{u}}_{\mathrm{AF}}$ lay in the film's plane and that $\hat{\mathbf{u}}_{\mathrm{FM}}$ and $\hat{\mathbf{u}}_{\mathrm{AF}}$ are parallel. In our simulations, noncollinearity between the $\hat{\mathbf{u}}_{\mathrm{FM}}$ and $\hat{\mathbf{u}}_{\mathrm{AF}}$ vectors has been allowed.[19,20,23,26]

In the framework of this model, rotatable anisotropy has not been originally considered. This anisotropy comes from interfacial AF spins that, due to sufficiently strong exchange interaction with the FM, can rotate simultaneously with the latter thus contributing to the enhancement of its coercivity. In order to explain the isotropic FMR shift, McMichael *et al.*[10] included an *unidirectional* rotatable anisotropy term of a form $-\mathbf{M}_{\mathrm{FM}}\cdot\mathbf{H}_{\mathrm{RA}}$. When irreversible magnetization processes are involved, however, rotatable anisotropy term proportional to $-(\mathbf{M}_{\mathrm{FM}}\cdot\mathbf{H})^2$ like ours should be considered in the model in order to reproduce both descending and ascending branches of a hysteresis loop trace.[23] The reason is that the coupling with these rotatable AF spins is sensed by the FM as an additional uniaxial anisotropy with symmetry axis always parallel to $\mathbf{H}$. Such phenomenological approach explains both the isotropic negative FMR shift and the increased coercivity in exchange-coupled bilayers with polycrystalline AF.[3,10,23] Similarly, when a variation in the so-called AF-induced canted uniaxial anisotropy[43] due to rotation processes in partly unstable AF grains is assumed, it results in coercivity variations.

Frequently, it is convenient to express the magnetic parameters in terms of effective fields. One of them is the exchange coupling field H_E, usually defined as $H_E = J_E/(t_{\mathrm{FM}}M_{\mathrm{FM}})$. For the energy expression under consideration, the other effective fields are the AF domain-wall anisotropy field $H_W=\sigma_W/(t_{\mathrm{FM}}M_{\mathrm{FM}})$, where σ_W is the energy per unit surface of a 90° AF domain wall, the FM uniaxial anisotropy field $H_U=2K_{\mathrm{FM}}/M_{\mathrm{FM}}$, and the rotatable anisotropy field $H_{\mathrm{RA}}=2K_{\mathrm{RA}}/M_{\mathrm{FM}}$. For in-plane $\mathbf{H}$, $\hat{\mathbf{u}}_{\mathrm{FM}}$, and $\hat{\mathbf{u}}_{\mathrm{AF}}$, the normalized free energy $\eta=E/(t_{\mathrm{FM}}M_{\mathrm{FM}})$ becomes

$$\eta = 2\pi(\mathbf{M}_{\mathrm{FM}}\cdot\hat{\mathbf{n}})^2 - H\cos(\phi_H-\phi_{\mathrm{FM}}) - \frac{1}{2}H_U\cos^2\phi_{\mathrm{FM}} - H_W\cos\phi_{\mathrm{AF}} - H_E\cos(\phi_{\mathrm{AF}}-\phi_{\mathrm{FM}}) - \frac{1}{2}H_{\mathrm{RA}}\cos^2(\phi_H-\phi_{\mathrm{FM}}),$$

where ϕ_H, ϕ_{FM}, and ϕ_{AF} are the angles that $\mathbf{H}$, $\mathbf{M}_{\mathrm{FM}}$, and $\mathbf{M}_{\mathrm{AF}}$, respectively, form with the easy axis.

APPENDIX B: TEMPERATURE DEPENDENCE OF H_E/H_W

Theoretical temperature dependencies of H_E and H_W can be obtained as follows. Assuming that $M_{\mathrm{AF}}(T)\propto(1-T/T_N)^{1/3}$ and that $H_E(T)$ varies as the AF magnetization[44,45] results in $H_E(T)=H_E(0)(1-T/T_N)^{1/3}$, where T_N is the Néel temperature of the AF. Also, if[38] $K_{\mathrm{AF}}(T)\propto M^3_{\mathrm{AF}}(T)$ then

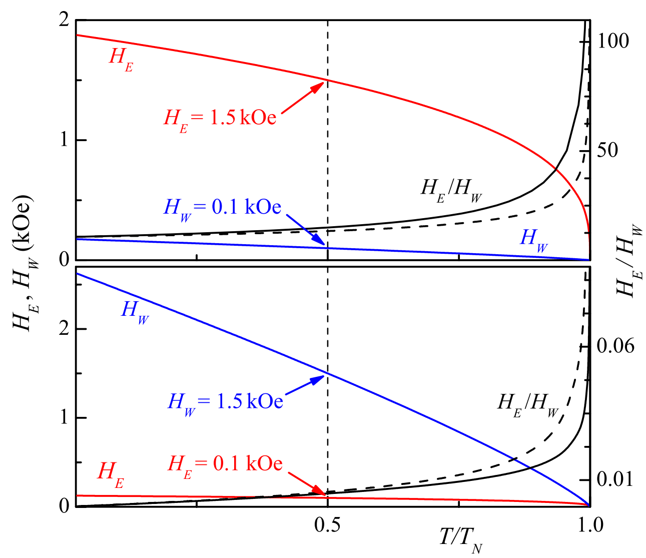

FIG. 4. (Color online) Temperature dependencies of H_E, H_W, and H_E/H_W for $H_E>H_W$ (top) and $H_E<H_W$ (bottom). The solid lines are calculated assuming $H_W(T)\propto(1-T/T_N)^{5/6}$ and $H_E(T)\propto(1-T/T_N)^{1/3}$, while the dashed lines for H_E/H_W are obtained using $H_E(T)\propto(1-T/T_N)^{1/2}$ (see the main text). Numerically, H_E and H_W are chosen in a way that at $T=T_N/2$ they equal those used in Fig. 1.

$H_W(T) = H_W(0)(1 - T/T_N)^{5/6}$ so one obtains $H_E(T)/H_W(T) \propto (1 - T/T_N)^{-1/2}$. The temperature dependencies of H_E, H_W, and H_E/H_W thus calculated are plotted in Fig. 4 for $H_E > H_W$ and $H_E < H_W$.

Alternatively, assuming[7] $H_E(T) \propto (1 - T/T_N)^{1/2}$ results in $H_E(T)/H_W(T) \propto (1 - T/T_N)^{-1/3}$. The corresponding H_E, H_W, and H_E/H_W variations with T are given by the dashed lined in Fig. 4.

[1] W. H. Meiklejohn and C. P. Bean, Phys. Rev. **102**, 1413 (1956); **105**, 904 (1957).
[2] W. H. Meiklejohn, J. Appl. Phys. **33**, 1328 (1962).
[3] J. Nogués and I. K. Schuller, J. Magn. Magn. Mater. **192**, 203 (1999).
[4] A. E. Berkowitz and K. Takano, J. Magn. Magn. Mater. **200**, 552 (1999).
[5] M. Kiwi, J. Magn. Magn. Mater. **234**, 584 (2001).
[6] J. Nogués, J. Sort, V. Langlais, V. Skumryev, S. Suriñach, J. S. Muñoz, and M. D. Baró, Phys. Rep. **422**, 65 (2005).
[7] A. P. Malozemoff, J. Appl. Phys. **63**, 3874 (1988).
[8] B. H. Miller and E. Dan Dahlberg, Appl. Phys. Lett. **69**, 3932 (1996); E. D. Dahlberg, B. Miller, B. Hill, B. J. Jönsson, V. Ström, K. V. Rao, J. Nogués, and I. K. Schuller, J. Appl. Phys. **83**, 6893 (1998).
[9] V. Ström, B. J. Jönsson, K. V. Rao, and E. D. Dahlberg, J. Appl. Phys. **81**, 5003 (1997); J. Åkerman, V. Ström, K. V. Rao, and E. D. Dahlberg, Phys. Rev. B **76**, 144416 (2007).
[10] R. D. McMichael, M. D. Stiles, P. J. Chen, and W. F. Egelhoff, Jr., Phys. Rev. B **58**, 8605 (1998).
[11] T. Pokhil, S. Mao, and A. Mack, J. Appl. Phys. **85**, 4916 (1999).
[12] P. Miltényi, M. Gruyters, G. Güntherodt, J. Nogués, and I. K. Schuller, Phys. Rev. B **59**, 3333 (1999).
[13] H. Xi, R. M. White, and S. M. Rezende, Phys. Rev. B **60**, 14837 (1999).
[14] J. Geshev, Phys. Rev. B **62**, 5627 (2000).
[15] J. R. Fermin, M. A. Lucena, A. Azevedo, F. M. de Aguiar, and S. M. Rezende, J. Appl. Phys. **87**, 6421 (2000).
[16] J. Geshev, L. G. Pereira, and J. E. Schmidt, Phys. Rev. B **64**, 184411 (2001).
[17] R. L. Rodríguez-Suárez, L. H. Vilela Leão, F. M. de Aguiar, S. M. Rezende, and A. Azevedo, J. Appl. Phys. **94**, 4544 (2003).
[18] J. Geshev, L. G. Pereira, J. E. Schmidt, L. C. C. M. Nagamine, E. B. Saitovitch, and F. Pelegrini, Phys. Rev. B **67**, 132401 (2003).
[19] J. Geshev, S. Nicolodi, L. G. Pereira, L. C. C. M. Nagamine, J. E. Schmidt, C. Deranlot, F. Petroff, R. L. Rodríguez-Suárez, and A. Azevedo, Phys. Rev. B **75**, 214402 (2007).
[20] J. Geshev, S. Nicolodi, L. G. Pereira, J. E. Schmidt, V. Skumryev, S. Suriñach, and M. D. Baró, Phys. Rev. B **77**, 132407 (2008).
[21] D. Mauri, H. C. Siegmann, P. S. Bagus, and E. Kay, J. Appl. Phys. **62**, 3047 (1987).
[22] H. Xi and R. M. White, Phys. Rev. B **61**, 80 (2000).
[23] J. Geshev, L. G. Pereira, and J. E. Schmidt, Phys. Rev. B **66**, 134432 (2002).
[24] L. C. C. M. Nagamine, J. E. Schmidt, M. N. Baibich, E. B. Saitovitch, and J. Geshev, Physica B **384**, 132 (2006).
[25] M. Ali, C. H. Marrows, and B. J. Hickey, Phys. Rev. B **67**, 172405 (2003).
[26] S. Nicolodi, L. C. C. M. Nagamine, A. D. C. Viegas, J. E. Schmidt, L. G. Pereira, C. Deranlot, F. Petroff, and J. Geshev, J. Magn. Magn. Mater. **316**, e97 (2007).
[27] F. Offi, W. Kuch, and J. Kirschner, Phys. Rev. B **66**, 064419 (2002).
[28] Y. Endoh and Y. Ishikawa, J. Phys. Soc. Jpn. **30**, 1614 (1961).
[29] F. Y. Yang and C. L. Chien, Phys. Rev. Lett. **85**, 2597 (2000).
[30] S. Roy, M. R. Fitzsimmons, S. Park, M. Dorn, O. Petracic, I. V. Roshchin, Z.-P. Li, X. Batlle, R. Morales, A. Misra, X. Zhang, K. Chesnel, J. B. Kortright, S. K. Sinha, and I. K. Schuller, Phys. Rev. Lett. **95**, 047201 (2005).
[31] M. R. Fitzsimmons, B. J. Kirby, S. Roy, Z.-P. Li, I. V. Roshchin, S. K. Sinha, and I. K. Schuller, Phys. Rev. B **75**, 214412 (2007).
[32] T. Ambrose and C. L. Chien, Phys. Rev. Lett. **76**, 1743 (1996); J. Appl. Phys. **83**, 6822 (1998).
[33] J. Saha, J. S. Parker, B. T. Bolon, A. Abin-Fuentes, C. Leighton, and R. H. Victora, J. Appl. Phys. **102**, 073901 (2007).
[34] L. E. Fernandez-Outon, G. Vallejo-Fernandez, S. Manzoor, B. Hillebrands, and K. O'Grady, J. Appl. Phys. **104**, 093907 (2008).
[35] L. E. Vallejo-Fernandez, L. E. Fernandez-Outon, and K. O'Grady, Appl. Phys. Lett. **91**, 212503 (2007).
[36] J.-V. Kim and R. L. Stamps, Phys. Rev. B **71**, 094405 (2005); Appl. Phys. Lett. **79**, 2875 (2001).
[37] J. Ben Youssef, V. Castel, K. Garello, N. Gargam, S. Pogossian, D. Spenato, D. T. Dekadjevi, A. Suvorova, T. R. Charlton, R. M. Dalgliesh, and S. Langridge, Phys. Rev. B **76**, 134401 (2007).
[38] M. D. Stiles and R. D. McMichael, Phys. Rev. B **60**, 12950 (1999); **63**, 064405 (2001).
[39] C. Leighton, J. Nogués, B. J. Jönsson-Åkerman, and I. K. Schuller, Phys. Rev. Lett. **84**, 3466 (2000).
[40] V. S. Spcriosu, D. A. Herman, I. L. Sanders, and T. Yogi, IBM J. Res. Dev. **34**, 884 (1990); S. S. P. Parkin and V. S. Speriosu, *Magnetic Properties of Low-Dimensional Systems II*, Springer Proceedings in Physics Vol. 50 (Springer, New York, 1990), p. 110.
[41] J. Seifert, T. Bernhard, M. Gruyters, and H. Winter, Phys. Rev. B **76**, 224405 (2007).
[42] R. Jungblut, R. Coehoorn, M. T. Johnson, J. aan de Stegge, and A. Reinders, J. Appl. Phys. **75**, 6659 (1994).
[43] J. McCord, C. Hamann, R. Schäfer, L. Schultz, and R. Mattheis, Phys. Rev. B **78**, 094419 (2008).
[44] E. Fulcomer and S. H. Charap, J. Appl. Phys. **43**, 4190 (1972).
[45] M. R. Fitzsimmons, C. Leighton, A. Hoffmann, P. C. Yashar, J. Nogués, K. Liu, C. F. Majkrzak, J. A. Dura, H. Fritzsche, and I. K. Schuller, Phys. Rev. B **64**, 104415 (2001).